Conductivity in a magnetic field of a three-dimensional composite with a random fractal structure

Vitaly V. Novikov and Dmitry Y. Zubkov
Odessa National Polytechnical University, 1 Shevchenko Prospekt, 65044 Odessa, Ukraine
(Received 18 April 2005; revised manuscript received 12 December 2005; published 22 February 2006)

Effective Hall properties of three-dimensional two-component disordered composite have been calculated. Our evaluations are based on ideas of renormalization group transformations, a fractal structure model, and an iterative averaging method. For the critical exponents of Hall coefficient t_1 ($p<p_c$) and s_1 ($p>p_c$) the following approximate values were obtained for various magnetic fields H: $H\to 0$, $1.8\leqslant t_1\leqslant 2.2$, $1.2\leqslant s_1\leqslant 2.2$; $H=10^2$, $0\leqslant t_1\leqslant 0.2$, $0.8\leqslant s_1\leqslant 2$; and $H\to\infty$, $s_1\simeq t_1\simeq 0$. Our results show agreement both with theoretical results (within the framework of effective medium theory, percolation theory) and with experimental data. It was shown that the calculations based on the iterative averaging method reveal agreement with the effective medium theory in the large interval of conductivity ratio: $1\geqslant\sigma_2/\sigma_1\geqslant 10^{-2}$ and with the percolation theory when conductivity ratio tends to zero: $\sigma_2/\sigma_1\to 0$.

DOI: 10.1103/PhysRevB.73.054202 PACS number(s): 72.20.−i, 72.70.+m, 05.40.−a

I. INTRODUCTION

The effective conductivity evaluation for a disordered medium is a sufficiently complicated problem that is of interest both in theoretical and experimental studies. A fundamental and satisfactory solution to the effective conductivity evaluation problem has been obtained within the framework of percolation theory for the metal (with conductivity σ_1)-nonmetal (with conductivity σ_2) composite when there is no magnetic field ($\mathbf{H}=0$) and the conductivity ratio (ratio of the components conductivities) tends to zero ($\sigma_2/\sigma_1\to 0$):[1]

$$\sigma_0\sim(p-p_c)^t,\quad p>p_c,$$

$$\sigma_0\sim(p_c-p)^{-s},\quad p<p_c, \tag{1}$$

where p is the concentration of the metallic component (σ_1) and p_c is the percolation threshold. The index "0" means that the magnetic field equals zero ($\mathbf{H}=0$). The critical exponents of conductivity (t,s) in the two- and three-dimensional cases according to Ref. 1 have such approximate values:

$$t\simeq 1.3,\quad s\simeq 0.5\quad (d=2),$$

$$t\simeq 1.6,\quad s\simeq 0.62\quad (d=3). \tag{2}$$

When the conductivity ratio is in the range $1>\sigma_2/\sigma_1>10^{-2}$ the effective properties of randomly inhomogeneous composite can be satisfactorily described by the effective medium theory:[2]

$$\sigma_0=\sigma_1 f(x,p),\quad x=\frac{\sigma_2}{\sigma_1},\quad f(x,p)=a+\left(a^2+\frac{1}{2}x\right)^{1/2},$$

$$a=\frac{1}{2}\left[\left(\frac{3}{2}p-\frac{1}{2}\right)(1-x)+\frac{1}{2}x\right]. \tag{3}$$

Thorough analysis of previous works revealed no adequate theory, which would describe the effective conductivity for the range of the conductivity ratio $0<\sigma_2/\sigma_1<10^{-2}$. The solution to the problem of evaluating the effective conductivity for disordered composite becomes even more complicated over a nonzero magnetic field ($\mathbf{H}\neq 0$).

Researchers made a number of attempts[3,4] to analyze the galvanomagnetic properties of inhomogeneous medium. The effective conductivity tensor $\hat{\sigma}$ was introduced in order to evaluate the effective galvanomagnetic properties:

$$\langle\mathbf{j}\rangle=\hat{\sigma}\langle\mathbf{E}\rangle,$$

$$\hat{\sigma}=\begin{vmatrix}\sigma_{11} & \sigma_{12} & 0\\ -\sigma_{12} & \sigma_{22} & 0\\ 0 & 0 & \sigma_{33}\end{vmatrix}. \tag{4}$$

The angular brackets mean the average over a volume V:

$$\langle\mathbf{j}\rangle=\frac{1}{V}\int\mathbf{j}(\mathbf{r})d^3r,\quad \langle\mathbf{E}\rangle=\frac{1}{V}\int\mathbf{E}(\mathbf{r})d^3r, \tag{5}$$

where $\mathbf{j}(\mathbf{r})$ and $\mathbf{E}(\mathbf{r})$ are the random functions of the coordinates. Suppose that Ohm's law is locally satisfied, so that

$$\mathbf{j}(\mathbf{r})=\hat{\sigma}(\mathbf{r})\mathbf{E}(\mathbf{r}),$$

$$\hat{\sigma}(\mathbf{r})=\begin{vmatrix}\sigma_{11}(\mathbf{r}) & \sigma_{12}(\mathbf{r}) & 0\\ -\sigma_{12}(\mathbf{r}) & \sigma_{22}(\mathbf{r}) & 0\\ 0 & 0 & \sigma_{33}(\mathbf{r})\end{vmatrix}. \tag{6}$$

The conductivity tensor $\hat{\sigma}(\mathbf{r})$ may then be expressed as

$$\hat{\sigma}_{ij}(\mathbf{r})=\hat{\sigma}^s_{ij}(\mathbf{r})+\hat{\sigma}^a_{ij}(\mathbf{r}),$$

where $\hat{\sigma}^s_{ij}(\mathbf{r})$ is the symmetric part of the conductivity tensor $[\hat{\sigma}^s_{ij}(\mathbf{r})=\hat{\sigma}^s_{ji}(\mathbf{r})]$ and $\hat{\sigma}^a_{ij}(\mathbf{r})$ is the antisymmetric part of the tensor $[\hat{\sigma}^a_{ij}(\mathbf{r})=-\hat{\sigma}^a_{ji}(\mathbf{r})]$.

A field notation Ohm's law in such a medium is

$$\mathbf{j}+\mathbf{j}\times\beta(\mathbf{r})=\sigma_0(\mathbf{r})\mathbf{E}, \tag{7}$$

where $\beta(\mathbf{r})=\beta(r)\mathbf{n}$ is the Hall parameter which is directed along the magnetic field $\mathbf{H}=H\mathbf{n}$. Relations between the Hall coefficient R, the Hall parameter β, the mobility μ, and the

density n of carriers with charge e look as follows:

$$R = -\frac{\beta}{\sigma H} = \frac{\mu}{\sigma} = \frac{1}{en}. \tag{8}$$

From the above expression we can make certain conclusions, which provide physical insight to the Hall coefficient R and the Hall parameter β:

$$R \sim n^{-1}, \quad \beta \sim -\mu. \tag{9}$$

Let y be the mobility ratio (the ratio of the mobilities of components) like x in Eq. (3):

$$y = \frac{\mu_2}{\mu_1}. \tag{10}$$

From Eqs. (9) and (10) it follows that

$$\frac{\beta_2}{\beta_1} = y; \quad \frac{R_2}{R_1} = \frac{n_1}{n_2} = \frac{y}{x}. \tag{11}$$

In other words, we can express any ratio of the Hall properties through two parameters: conductivity ratio x and mobility ratio y.

The conductivity tensor $\hat{\sigma}(\mathbf{r})$ according to Eqs. (6) and (7) will then read

$$\hat{\sigma}(\mathbf{r}) = \frac{\sigma_0(\mathbf{r})}{1+\beta^2(\mathbf{r})} \begin{vmatrix} 1 & -\beta(\mathbf{r}) & 0 \\ \beta(\mathbf{r}) & 1 & 0 \\ 0 & 0 & 1+\beta^2(\mathbf{r}) \end{vmatrix}. \tag{12}$$

This tensor satisfactorily describes the conductivity of noncompensated metals and semiconductors.

The first successful attempt to get an exact solution for the effective Hall properties of a composite was made in Refs. 5 and 6. Authors acting independently of each other have given a computational method for the effective Hall properties for two-dimensional two-phase systems with statistically equivalent and isotropic allocations of the first and second phase ($p_1 = p_2 = 0.5$).

It was supposed that each of the phases is characterized by two parameters: the ohmic conductivity $\sigma_0(\mathbf{r})$ and the Hall factor $\beta(\mathbf{r})$. However, each of the properties $\sigma_0(\mathbf{r})$ and $\beta(\mathbf{r})$ from conductivity tensor (12) accepts only two values: $\sigma_0 = \sigma_1$ and $\beta = \beta_1$ in the first phase, and $\sigma_0 = \sigma_2$ and $\beta = \beta_2$ in the second phase. The essence of ideas described in Refs. 5 and 6 revolves around linear transformations from the old fields $(\mathbf{j}, \mathbf{E})$ to new fields $(\mathbf{j}', \mathbf{E}')$. The macroscopic properties of the new system are equivalent to those of the original system. These transformations can be applied only to a two-dimensional system (extendable to a case of columnar microstructure[7]), since in such case they do not change the laws governing a direct current, namely

$$\mathbf{j} = b\mathbf{n} \times \mathbf{E}, \quad \mathbf{E} = d\mathbf{n} \times \mathbf{j}, \tag{13}$$

$$\mathbf{j}' = a'\mathbf{j}'' + b'\mathbf{n} \times \mathbf{E}'', \quad \mathbf{E}' = c'\mathbf{E}'' + d'\mathbf{n} \times \mathbf{j}''. \tag{14}$$

The transformations (13) and (14) allow one to calculate the effective galvanomagnetic properties of two-dimensional (2D) inhomogeneous medium when only the conductivity fluctuates and the Hall factors of both components are equal, i.e., $\sigma_1 \neq \sigma_2$, $\beta_1 = \beta_2$.[5,6] If we apply a requirement of complementarity, i.e., in the first phase (σ_1, β_1) we have $\sigma' = \sigma_2$, $\beta' = -\beta_2$, and in the second phase (σ_2, β_2) we have $\sigma' = \sigma_1$, $\beta' = -\beta_1$ then we shall obtain the following results for the effective Hall properties:

$$\sigma = \langle\sigma\rangle \left\{ \langle\sigma\rangle \left\langle \frac{1}{\sigma} \right\rangle + \beta_1^2 \left[\langle\sigma\rangle \left\langle \frac{1}{\sigma} \right\rangle - 1 \right] \right\}^{-1/2},$$

$$\beta = \beta_1 \left\{ \langle\sigma\rangle \left\langle \frac{1}{\sigma} \right\rangle + \beta_1^2 \left[\langle\sigma\rangle \left\langle \frac{1}{\sigma} \right\rangle - 1 \right] \right\}^{-1/2}. \tag{15}$$

Here the symbol "$\langle\ \rangle$" means volume average. The transformations (13) and (14) led to a result for another case, when only the Hall parameter fluctuates, however, the conductivities of the components are equal, i.e., $\sigma_1 = \sigma_2$, $\beta_1 \neq \beta_2$.[5,6]

In Ref. 8 the solution for the more general case ($\sigma_1 \neq \sigma_2$, $\beta_1 \neq \beta_2$) has been obtained. It was given by inserting the additional coefficients to the transformation (13):

$$\mathbf{j} = a\mathbf{j}' + b\mathbf{n} \times \mathbf{E}', \quad \mathbf{E} = c\mathbf{E}' + d\mathbf{n} \times \mathbf{j}'.$$

This transformation in Ref. 8 led to the following results for the effective Hall properties:

$$\sigma = \sqrt{\frac{\sigma_1\sigma_2}{1 + (\sigma_1\beta_2 - \sigma_2\beta_1)^2/(\sigma_1^2 + \sigma_2^2)}},$$

$$\beta = \sigma\frac{\beta_1 + \beta_2}{\sigma_1 + \sigma_2}. \tag{16}$$

It is interesting to note that in the absence of a magnetic field ($\beta_1 = \beta_2 = 0$) both Eqs. (15) and (16) lead to the classical result $\sigma = \sqrt{\sigma_1\sigma_2}$.

The above approach is known as Keller-Dykhne method. It is a powerful tool in many studies of the transport problem. Therefore it is no surprise that attempts were made to extend it in various ways,[9,10,7] including even application to the fractional quantum Hall effect.[11] Particularly, numerical computations for a 2D composite were carried out in Ref. 9. Furthermore, new perturbation analysis was proposed in Ref. 10 and a composite with a columnar microstructure was studied in Ref. 7.

The behavior of Hall coefficient near the percolation threshold p_c in a composite containing a dielectric and metallic phase has been studied in Ref. 1 for

$$\beta_1 = \beta_2, \quad \frac{R_1}{R_2} = \frac{\sigma_2}{\sigma_1} \ll 1.$$

Two concentration value regions were considered: before and after the percolation threshold. The behavior of the effective Hall coefficient for $\Delta \ll p - p_c \ll 1$ was described by the following power dependence:

$$R(p) = R_1(p - p_c)^{-s_1}, \quad p > p_c, \tag{17}$$

where s_1 is a critical exponent for the Hall coefficient. $s_1 = 0$ for two-dimensional medium ($d = 2$) and $s_1 = 0.9$ for three dimensions ($d = 3$).

For $1 \gg p_c - p \gg \Delta$ the effective Hall coefficient was described by another power dependence:

$$R(p) = R_2(p_c - p)^{t_1}, \quad p_c > p, \tag{18}$$

where t_1 is the critical exponent of the Hall coefficient: $t_1 \simeq 1.1$, $d=2$; $t_1 \simeq 1.62$, $d=3$.[1]

The author of Ref. 12 provided the first quantitative test of the random resistor network model. Resistor networks, from which resistors are removed at random, provide the natural generalization of the lattice models for which percolation thresholds and percolation probabilities have previously been considered. Except close to threshold, Monte Carlo data for the models based on bond percolation give good agreement with a simple effective medium theory, which can also treat continuous media. In Ref. 13 the authors employed the random resistor network model to determine behavior of low-field Hall effect in a 3D "metal-nonmetal" composite near the percolation threshold. Note that such an approach[12,13] gives satisfactory approximate results when $p_c < p \leqslant 1$. For the following power laws for effective values of ohmic conductivity σ, Hall coefficient R, and Hall conductivity σ_{12} the authors[13] obtained the critical exponents:

$$\sigma/\sigma_1 \sim (p - p_c)^t, \quad R/R_1 \sim (p - p_c)^{-s_1},$$

$$\sigma_{12}/\sigma_{12}^{(1)} \sim (p - p_c)^{t_2}, \quad p > p_c,$$

$$p_c = 0.2465, \quad t = 1.64 \pm 0.04,$$

$$s_1 = 0.29 \pm 0.05, \quad t_2 = 3.0 \pm 0.1, \tag{19}$$

where t_2 is the critical exponent for the Hall conductivity σ_{12}. However, authors[14] found that in three dimensions the effective conductivity obeys a quadratic law $\sigma(p) \sim (p - p_c)^2$, so that $t=2$.

Further, such scaling assumptions were made by the authors of Ref. 13 in their subsequent publication:[15]

$$\frac{\sigma_{12} - \sigma_{12}^{(1)}}{\sigma_{12}^{(2)} - \sigma_{12}^{(1)}} = |p - p_c|^{t_2} F_{\sigma_{12}}(Z), \quad \frac{\sigma - \sigma_1}{\sigma_2 - \sigma_1} = |p - p_c|^t F_\sigma(Z),$$

$$\frac{\sigma_2}{\sigma_1} \ll 1, \quad |p - p_c| \ll 1, \quad Z = \frac{\sigma_2/\sigma_1}{|p - p_c|^{t+s}}, \tag{20}$$

where $F_{\sigma_{12}}$, F_σ are the scaling functions with scaling argument Z. This time in Ref. 15 a more accurate value of the conductivity critical exponent has been used, namely $t = 1.95$. A similar approach was applied in Ref. 16 to describe the behavior of a three-constituent metal-insulator-superconductor composite.

The authors in Ref. 17 studied the multifractal properties of the current distribution of the three-dimensional random resistor network at the percolation threshold. Measuring the second, the fourth, and the sixth moments of the current distribution allowed them to find that $t \simeq 2.01$. The author of Ref. 18 reported such a result for a three-dimensional simple cubic lattice: $t = 2.14 \pm 0.02$, and quoted such a result for the critical exponent s: $s = 0.9 \pm 0.1$.

In Ref. 19 it was argued that in carbon-black polymer composites long-range interactions could drive the system towards the mean-field regime for which $t=3.0$.

The authors of Ref. 2 used the following formulas obtained by combining formulas of the effective medium theory with formulas of the percolation theory to calculate the effective Hall properties of a composite:

$$\sigma_0/\sigma_1 = (1 - p/p_c)^{-1},$$

$$R/R_1 = (y/x)(1 - p/p_c)^2 + (3 - p/p_c)^2(1 - xy)p,$$

$$\mu/\mu_1 = y(1 - p/p_c)^2 + x(3 - p/p_c)^2(1 - p/p_c)^{-1}(1 - xy)p. \tag{21}$$

Here concentration p_c is the percolation probability $p_c = 1/3$; μ the Hall mobility; $x = \sigma_2/\sigma_1$ the conductivity ratio; and $y = \mu_2/\mu_1$ the mobility ratio of the components. These formulas describe the behavior of the effective properties satisfactorily only in the concentration range $0.4 < p < 1$.

The authors of Ref. 20 studied the effective medium theory approximations for linear composite media by means of a path integral formalism. For the conductivity critical exponents they obtained $s=0$, $t=2$ in any spatial dimension $d \geqslant 2$. The perturbation theory for a 3D composite has been described in Refs. 3, 21, and 22. Note that both the effective medium theory and the perturbation theory more or less accurately describe the composite only in certain intervals of the components Hall properties and concentrations, where the corresponding assumptions are valid. It is essential, that if $\beta \gg 1$, then $\sigma_{12} \gg \sigma_{11}$ [see Eq. (12)]. Therefore even for small inhomogeneities, when σ_0 and β fluctuate weakly ($\delta\sigma_0/\sigma_0 \ll 1$, $\delta\beta/\beta \ll 1$), the fluctuation of $\sigma_{12} \sim \beta^{-1}$ is essential in comparison with $\sigma_{11} \sim \beta^{-2}$ and perturbation theory is not applicable. Note that when $\beta \gg 1$ the fluctuation of σ_{12} according to Eqs. (8) and (12) is caused by the fluctuation of density of carriers n.

From the above brief review it follows that the adequate theoretical model of galvanomagnetic properties of composites with random structure still does not exist for a three-dimensional case. We are not aware of any works where the influence of fractal and random structure of a 3D composite on the effective galvanomagnetic properties has been analyzed.

In the following section, the detailed analysis of effective Hall properties of a 3D two-component composite will be carried out based on the fractal structure model and the iterative averaging method.

II. FRACTAL STRUCTURE MODEL AND ITERATIVE AVERAGING METHOD

A lattice with a random distribution of parameters was chosen as an appropriate model of the chaotic structure of an inhomogeneous material. Spatial microinhomogeneities (i.e., system components) were modeled by the lattice junctions, and the interjunction bonds simulated their contacts with neighbors (see Fig. 1).

The main ensemble of bonds $\Omega_f(l,p)$ was obtained by means of the following iterative process. At the initial step ($k=0$) the finite lattice has an edge size l and probability p for a bond between neighboring lattice junctions to be un-

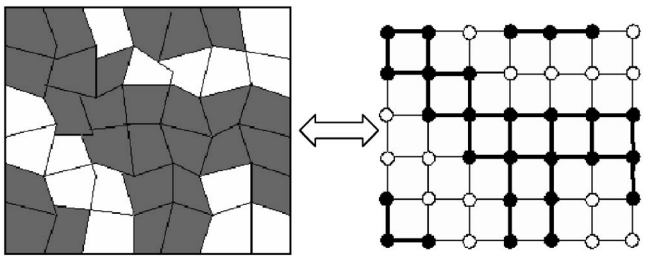

FIG. 1. Modeling of the chaotic structure of a composite.

broken (or "colored" with a definite color, so that bonds of the same color were assumed to have identical properties). For a two-component system it is convenient to choose two colors: black for the areas filled by a well conducting phase (σ_1,β_1) with concentration p and white for the bad conductor (σ_2,β_2) regions with concentration $(1-p)$. At the following steps $(k=1,2,\ldots,n)$ each bond of the lattice was replaced by a lattice generated at the previous step (Fig. 2). The scale of a lattice at the following steps is defined as

$$L_k = l^{k+1}. \tag{22}$$

The iteration process stops at the step $(k=n)$ when properties of the lattice do not depend on the number of iteration steps n. Consequently, the scale of a lattice equals $L_n=\xi$, where ξ is a correlation length. The set of bonds $\Omega_f(l,p)$ obtained by means of an iterative procedure depends on the size of an initial lattice l and a bulk concentration of black connections p.

There are two types of connection sets possible in a lattice: the connecting set and nonconnecting set of bonds. Formation of a connecting set is manifested by the presence in the set of complete (black) bonds connecting two opposite sides of the lattice. Formation of a nonconnecting set is manifested by the absence in the set of complete (black) bonds connecting two opposite sides. The probability $Y(p)$ of

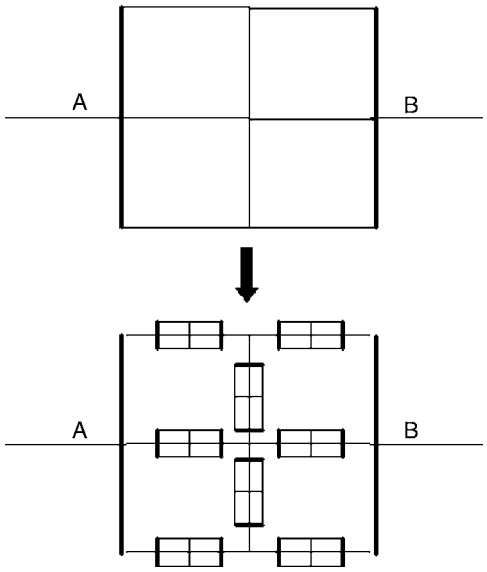

FIG. 2. Formation of the next iteration step.

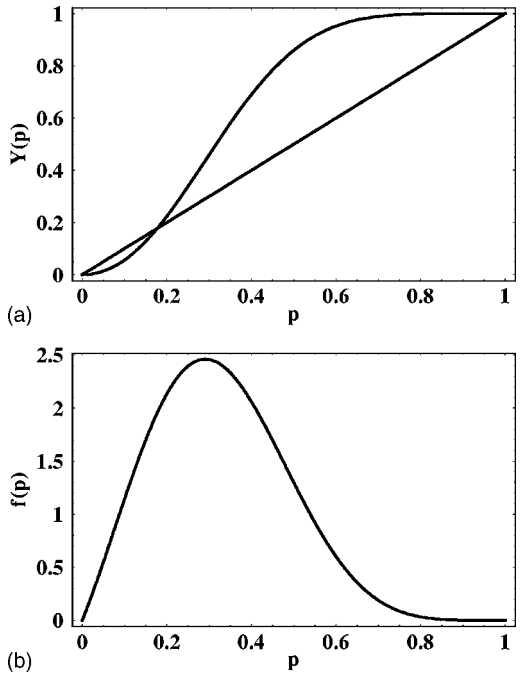

FIG. 3. Probability function $Y(p)$ and its derivative $f(p)$ for 3D rectangular lattice $(l=2)$. The intersection of the coordinate axes bisector $[Y(p)=p]$ with the curve $Y(p)$ defines the percolation threshold p_c.

connecting set formation was calculated as a relation of the connecting set number to a number of all possible configurations. Probability function $Y(p)$ for three-dimensional rectangular lattice $d=3$, $l=2$ was calculated by a similar method to Ref. 18 (see Fig. 3) and looks as follows:

$$\begin{aligned} Y(p) = {} & 5p^2(1-p)^{12} + 68p^3(1-p)^{11} + 398p^4(1-p)^{10} \\ & + 1298p^5(1-p)^9 + 2575p^6(1-p)^8 + 3288p^7(1-p)^7 \\ & + 2977p^8(1-p)^6 + 2000p^9(1-p)^5 + 1001p^{10}(1-p)^4 \\ & + 364p^{11}(1-p)^3 + 91p^{12}(1-p)^2 + 14p^{13}(1-p) + p^{14}. \end{aligned} \tag{23}$$

The percolation threshold p_c can be calculated from the following equation:

$$Y(p) = p.$$

The probability of nonconnecting set formation equals $[1-Y(p)]$. The relation between the probability function $Y(p)$ and the corresponding probability density $f(p)$ looks as

$$Y(p) = \int f(p)dp.$$

The value of the derivative of the function $Y(p)$ at a fixed point $p=p_c$ allows us to detect a type of the fixed point:

$$\left.\frac{dY(p)}{dp}\right|_{p=p_c} = \lambda,$$

if $\lambda<1$ then the fixed point $p=p_c$ is stable, if $\lambda>1$ then the fixed point $p=p_c$ is unstable.

The function $Y(p)$ [Eq. (23)] inside the interval (0, 1) has one fixed unstable point $p_c \simeq 0.178$ where $\lambda \simeq 1.958$. The point $p=p_c$ is a percolation threshold, i.e., a nonconnecting set transforms into a connecting set at $p \simeq 0.178$. Note that the probability function $Y(p)$ becomes more complicated for a larger 3D lattice. To our knowledge the function $Y(p)$ has no analytical expression like Eq. (23) already for $l=3$ as of yet.

Now, if we know the values of the λ and the unit cell size l, we can calculate the critical exponent ν for the correlation length ξ:

$$\nu = \frac{\ln l}{\ln \lambda}. \tag{24}$$

The critical exponent ν defines the critical behavior of the correlation length as[23–25]

$$\xi \sim |p - p_c|^{-\nu}. \tag{25}$$

Hence at the first step of iterative process (zero step) the length of a lattice edge equals $L_0=l$. Hall properties of the first (black) component are $\sigma_{CS}^{(0)}=\sigma_1$, $\beta_{CS}^{(0)}=\beta_1$ and properties of the second (white) component are $\sigma_{NCS}^{(0)}=\sigma_2$, $\beta_{NCS}^{(0)}=\beta_2$. Bulk concentration of the "black" component equals p. At the next step of iteration process (first step) the length of lattice edge according to Eq. (22) equals $L_1=l^2$ and the bond concentration of the same color, for instance, black (σ_1, β_1), is $p_1=Y(p)$. At the following steps we have

$$p_2 = Y(p_1), \quad L_2 = l^3,$$

$$\ldots,$$

$$p_k = Y(p_{k-1}), \quad L_k = l^{k+1}. \tag{26}$$

Growth of the fractal random set $\Omega_f(l,p)$ of bonds stops at the kth step of iteration in fixed stable point 0 or 1 for function $p_k=Y(p_{k-1})$:

$$\lim_{k\to\infty} p_k = \begin{cases} 1, & p > p_c, \\ 0, & p < p_c. \end{cases} \tag{27}$$

Each of the bonds from the fractal random set $\Omega_f(l,p)$ at the kth step possesses the Hall properties (σ_k, β_k), namely, ohmic conductivity and a Hall parameter.

We now consider a two-phase 3D system with the distribution function similar to Ref. 18:

$$p(\sigma) = (1-p)\,\delta(\sigma - \sigma_2^{(0)}) + p\,\delta(\sigma - \sigma_1^{(0)}),$$

$$p(\beta) = (1-p)\,\delta(\beta - \beta_2^{(0)}) + p\,\delta(\beta - \beta_1^{(0)}), \tag{28}$$

where $\delta(x)$ is the Dirac delta function; p the probability that the actual local region possesses the following Hall properties: $\sigma_1^{(0)}=\sigma_1$, $\beta_1^{(0)}=\beta_1$; and $(1-p)$ the probability that the actual local region possesses other Hall properties: $\sigma_2^{(0)}=\sigma_2$, $\beta_2^{(0)}=\beta_2$.

After k iterative steps the distribution function will be

$$p(\sigma) = p\,\delta(\sigma - \sigma^{(k)}),$$

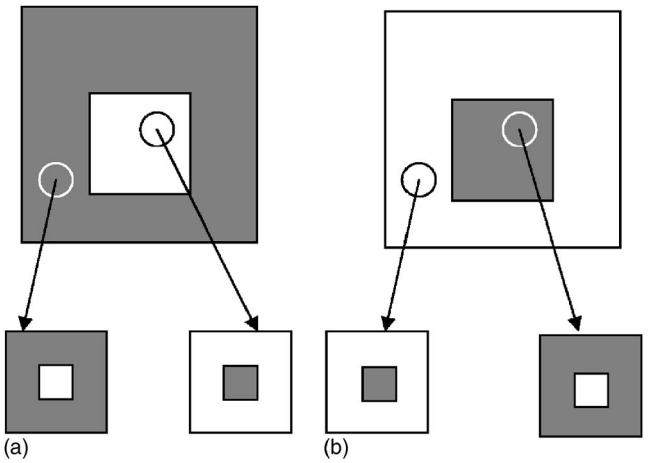

FIG. 4. Modeling of connecting and nonconnecting sets.

$$p(\beta) = p\,\delta(\beta - \beta^{(k)}),$$

and in the limit of large k we have the desired effective values

$$\lim_{k\to\infty} \sigma_{CS}^{(k)} = \lim_{k\to\infty} \sigma_{NCS}^{(k)} = \sigma,$$

$$\lim_{k\to\infty} \beta_{CS}^{(k)} = \lim_{k\to\infty} \beta_{NCS}^{(k)} = \beta. \tag{29}$$

III. RESULTS AND DISCUSSION

For the purpose of the calculation of the effective Hall properties of 3D composite the model of a cube inside a cube (see the Appendix) was applied. At each step of the iterative process evaluation of the Hall properties of connecting and nonconnecting set structures was carried out based on a rudimentary cell of a cube inside a cube. The continuous array from the well conducting (black) phase with a cube from a poorly conducting (white) phase inserted forms the connecting set [Fig. 4(a)], and continuous array from a poorly conducting (white) phase with a cube from a well conducting (black) phase inserted forms the nonconnecting set [Fig. 4(b)].

Hence at the kth iterative step, if $L_k < \xi$ (ξ is the correlation length) the composite has the self-similar random structure consisting of unit cells comprised of a cube inside a cube.

The calculations were made for a two-component 3D composite with random structure. First we shall consider the comparison of the result for the effective conductivity calculated by means of the iterative method with the calculation under formulas (3) obtained on the basis of effective medium theory model when $\mathbf{H}=0$.

Figure 5 shows the comparison between results for the effective conductivity obtained by means of the iterative method (continuous) and the calculation under the formula (3) obtained on the basis of the effective medium theory model (dashed). The comparison (Fig. 5) reveals their close agreement for the conductivity ratio $x=\sigma_2/\sigma_1 > 10^{-2}$. How-

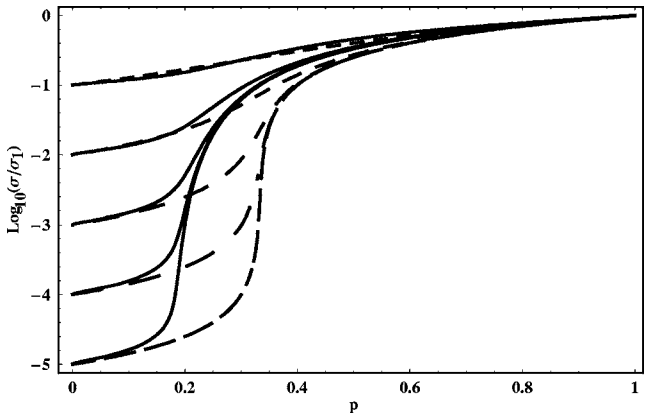

FIG. 5. The comparison of the calculations for the relative effective conductivity, obtained by effective medium theory and by means of the iterative method at various conductivity ratios $x = 10^{-5}$, 10^{-4}, 10^{-3}, 10^{-2}, and 10^{-1}.

ever, if $x \leqslant 10^{-2}$ the calculations show essential discrepancy when the concentration is $0.1 < p < 0.5$. This discrepancy grows as $x \to \infty$.

Figure 6 shows the comparison between the results for the effective conductivity obtained by means of the iterative method (continuous) calculation under formula (3) obtained on the basis of the effective medium theory model (dashed) and computational modeling.[2]

The comparison shows close agreement between the iterative method of computation (continuous) and the numerical experiment (dotted). There is an essential discrepancy between the self-consistent field approximation (dashed) and the numerical experiment (Fig. 6). The discrepancy of self-consistent field approximation (dashed) with the numerical experiment (Fig. 6) already has been observed in Ref. 2.

Hence the iterative method of computation is in close agreement with the effective medium theory model at $\sigma_2/\sigma_1 > 10^{-2}$ and coincides with the results of computational modeling at $\sigma_2/\sigma_1 \to 0$. It gives grounds to conclude that the iterative method satisfactorily describes the effective conductivity of a 3D composite with a random structure.

The analysis of effective conductivity for a 3D composite with a random structure becomes more complicated if $\mathbf{H} \neq 0$ because for $\mathbf{H}=0$ the effective conductivity depends on only two parameters: volume concentration p and conductivity ratio x of the components ($x=\sigma_2/\sigma_1$). If $\mathbf{H} \neq 0$, however, the effective conductivity as well as the effective Hall parameter depends on four parameters: (x,p) mentioned above, $\mathbf{H}$, and the mobility ratio $y=\mu_1/\mu_2$: $\sigma(p,H,x,y)$, $R(p,H,x,y)$.

Figure 7 shows results of calculations for the effective conductivity near the percolation threshold when the conductivities of components differ essentially, however, their Hall factors are equal ($x=10^{-10}$, $y=1$) for various values of the magnetic field H. We took such values of the Hall properties in order to focus on effects caused by the fluctuation of density of carriers n [Eqs. (8)–(11)]. If $\mathbf{H}=0$ [Fig. 7(a)] a "classic" cluster growth occurs in a composite when the bulk concentration of the first component increases from zero to the percolation threshold. Above the percolation threshold connecting sets of bonds exist in the composite and behavior of the medium is similar to the complete metallic phase (first component). However, if the magnetic field is nonzero [Figs. 7(b) and 7(c)], both below and above the percolation threshold conductivity decreases. If $\mathbf{H}=0$ in both components the carrier has a straight-line trajectory. The carrier passes the distance between collisions which is equal to free path l. If we apply the magnetic field $\mathbf{H} \neq 0$, then the trajectory of a carrier is a cycloid segment. The length of the segment is less than free path long because the carrier passes a lesser path in the same time τ between collisions; and so the drift speed and, consequently, mobility μ decreases, i.e., the conductivity in both components decreases. It was taken into account in Eq. (12) mathematically. As shown in Figs. 7(b) and 7(c), the magnetic field changes the sign of the power law (1) below the percolation threshold and does not change the character of the power law above the percolation threshold.

In order to describe the critical behavior of the galvanomagnetic properties quantitatively, we now define the logarithmic derivatives χ_σ, χ_R of the conductivity and of the Hall's coefficient as

$$\chi_\sigma(p,H,x,y) = \frac{\log_{10}[\sigma(p+\Delta p,H,x,y)] - \log_{10}[\sigma(p,H,x,y)]}{\log_{10}[p+\Delta p - p_c] - \log_{10}[p-p_c]},$$

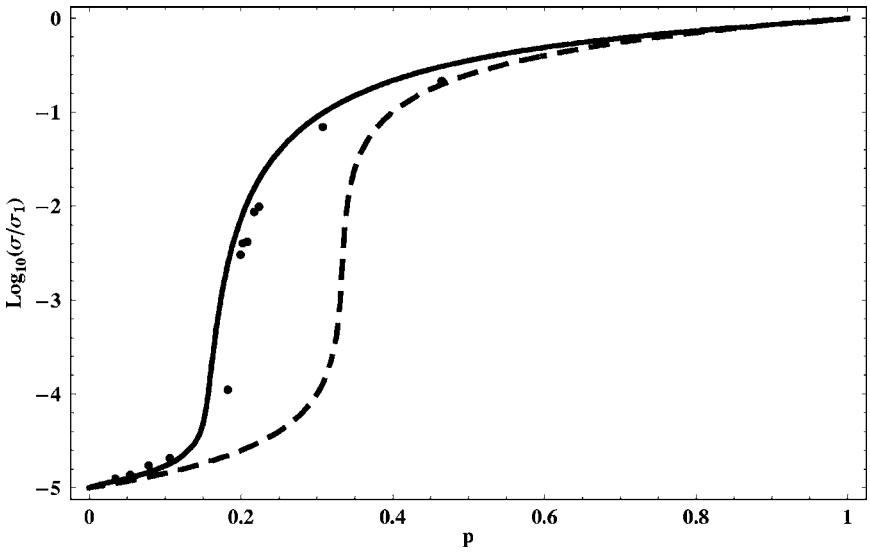

FIG. 6. The comparison of calculations for the relative effective conductivity, obtained by effective medium theory, by means of an iterative method and by the computational modeling for $x=10^{-5}$.

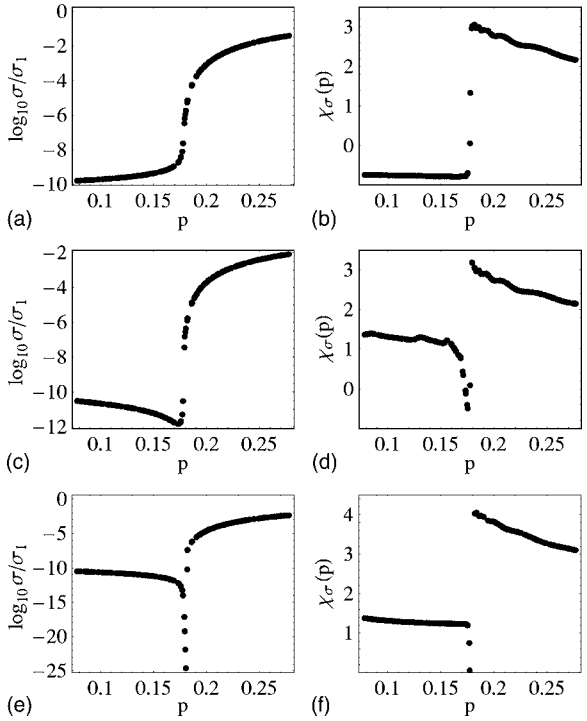

FIG. 7. The dependence of the relative effective conductivity (a), (c), (e) and the logarithmic derivative of effective conductivity (b), (d), (f) on concentration near the percolation threshold when the conductivities of components differ essentially but their Hall factors are equal ($x=10^{-10}$, $y=1$): (a) and (b) $H\to 0$; (c) and (d) $H=10^2$; and (e) and (f) $H\to\infty$.

$$\chi_R(p,H,x,y)=\frac{\log_{10}[R(p+\Delta p,H,x,y)]-\log_{10}[R(p,H,x,y)]}{\log_{10}[p+\Delta p-p_c]-\log_{10}[p-p_c]}.$$

We note again that the galvanomagnetic properties near the percolation threshold are described by the following dependencies:

$$\sigma\sim(p_c-p)^{-s}\quad \text{if } (p_c-p)>0,$$

$$\sigma\sim(p-p_c)^{t}\quad \text{if } (p-p_c)>0,$$

$$R\sim(p_c-p)^{t_1}\quad \text{if } (p_c-p)>0,$$

$$R\sim(p-p_c)^{-s_1}\quad \text{if } (p-p_c)>0.$$

The critical exponents t,s and t_1,s_1 may be obtained if we find the values of the functions χ_σ and χ_R at fixed x and y ($x=10^{-10}$, $y=1$) in the percolation limit ($p\to p_c$):

$$t(H)=\lim_{p\to p_c+0}\chi_\sigma(p,H),\quad t_1(H)=\lim_{p\to p_c+0}\chi_R(p,H),$$

$$s(H)=\lim_{p\to p_c-0}\chi_\sigma(p,H),\quad s_1(H)=\lim_{p\to p_c-0}\chi_R(p,H).$$

The calculations for the critical exponents from the above formulas for the dependencies of conductivity on concentration according to Fig. 7 give the following approximate values:

$$H\to 0,\quad 0.8\leqslant s\leqslant 0.9,\quad 2.2\leqslant t\leqslant 3;$$

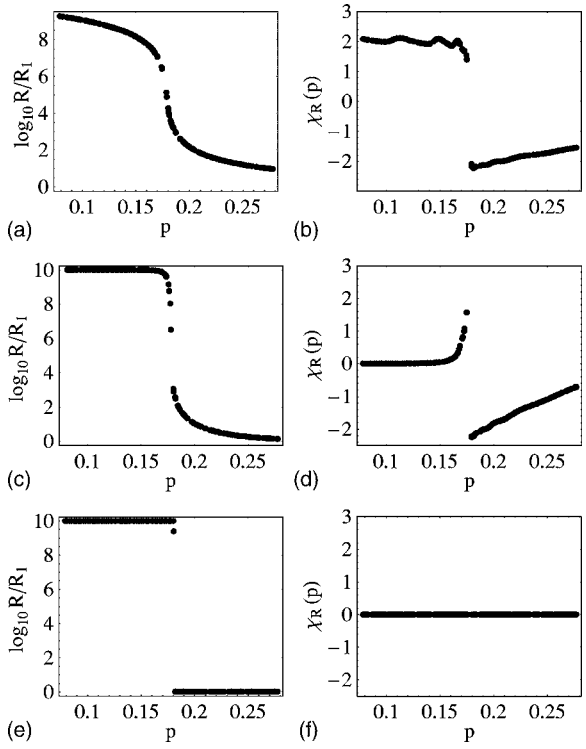

FIG. 8. The dependence of the relative Hall coefficient (a), (c), (e) and logarithmic derivative of the relative Hall coefficient (b), (d), (f) on concentration near the percolation threshold when the conductivities of components differ essentially, however, their Hall factors are equal ($x=10^{-10}$, $y=1$): (a) and (b) $H\to 0$; (c) and (d) $H=10^2$; and (e) and (f) $H\to\infty$.

$$H=10^2,\quad -1.4\leqslant s\leqslant -0.9,\quad 2.2\leqslant t\leqslant 3;$$

$$H\to\infty,\quad -1.2\leqslant s\leqslant -1.1,\quad 3\leqslant t\leqslant 4. \qquad (30)$$

Figure 8 shows the results of the calculations for the dependency of relative effective Hall coefficient on the bulk concentration of the first component near the percolation threshold at the same Hall properties of the components as in Fig. 7 ($x=10^{-10}$, $y=1$) for various values of magnetic field H. When there is no magnetic field, behavior of the Hall coefficient is described by power laws (17) and (18). It is easy to understand such a character of the dependency of relative effective Hall coefficient on the bulk concentration. If $\mu_1=\mu_2$, then from Eq. (8) we obtain the following relationship between dependencies in Figs. 7(a) and 8(a):

$$\frac{R_2}{R_1}=\frac{\sigma_1}{\sigma_2}.$$

However, if we apply the nonzero magnetic field, there is no dependency of relative effective Hall coefficient on concentration below the percolation threshold [Figs. 8(b) and 8(c)] because of decrease of the mobility, mentioned above. In this case we have [Eq. (8)]

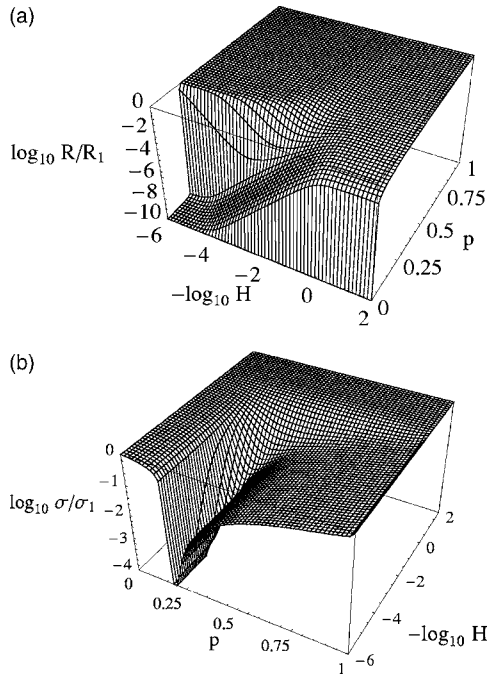

FIG. 9. The dependence of the relative effective Hall coefficient (a) and the relative effective conductivity (b) on the concentration and on the magnetic field when the Hall factors of components differ essentially, however, their conductivities are equal ($x=1$, $y=10^{-10}$).

$$\frac{R_2}{R_1} = \frac{\sigma_1 \mu_2}{\sigma_2 \mu_1}.$$

Evidently, the decrease of mobility compensates the conductivity increase.

According to the calculation of critical exponents from formulas (17) and (18) for the dependencies of the effective Hall coefficient on concentration (Fig. 8) the following approximate values were obtained:

$$H \to 0, \quad 1.8 \leqslant t_1 \leqslant 2.2, \quad 1.2 \leqslant s_1 \leqslant 2.2;$$

$$H = 10^2, \quad 0 \leqslant t_1 \leqslant 0.2, \quad 0.8 \leqslant s_1 \leqslant 2;$$

$$H \to \infty, \quad s_1 \simeq t_1 \simeq 0. \tag{31}$$

From the brief review in the previous section it follows that today the critical exponents t and s are thoroughly investigated in literature when $H=0$. The upper limits of the critical exponents in our calculations are slightly exceeded then those reported by most of the authors mentioned in the previous section. Hence our calculations in the percolation limit (near $p=p_c$) which correspond to the upper limits of the critical exponents can be considered as the analysis of the qualitative dependence of the effective Hall properties. The accuracy of the effective Hall properties calculation depends on the adequacy of the probability function $Y(p)$, the equations (A23) and (A25), and the actual structure of the inhomogeneous medium.

Figure 9 shows the results of calculation for the dependencies of the relative effective Hall coefficient Fig. 9(a) and the relative effective conductivity Fig. 9(b) on the bulk concentration of the first component when the values of conductivities of components are equal ($x=1$) and the Hall factor in the second component is very small ($\beta_2=10^{-10}\beta_1$, $y=10^{-10}$) for various values of the magnetic field H. We took such values of the Hall properties in order to focus on effects caused by the fluctuation of mobility of carriers μ [Eqs. (8)–(11)].

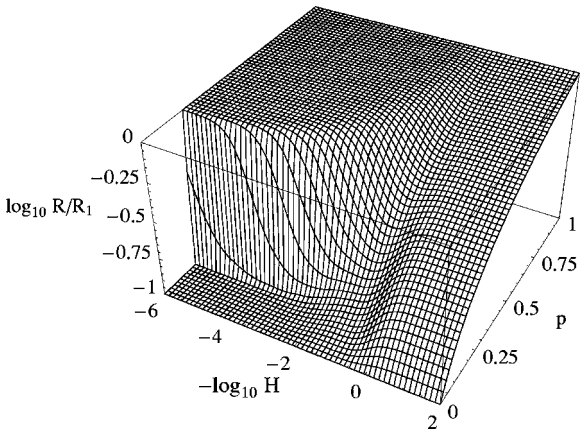

FIG. 10. The dependence of the relative effective Hall coefficient on the concentration and on the magnetic field when $x=1$, $y=0.1$.

The Hall coefficient sharply increases at small concentrations $p \simeq 0$ when $H=0$ (Fig. 9). Effective conductivity for this case does not depend on concentration (Fig. 9). When a magnetic field grows, the sudden jump of the Hall coefficient at $p \simeq 0$ departs from the percolation threshold $p=p_c$ [Fig. 9(a)]. Furthermore, in the dependence of the effective conductivity on magnetic field a minimum exists near the percolation threshold the depth of which tends to zero as $H \to \infty$ [Fig. 9(b)]. This is caused by the appearance of the rotating currents induced by the difference in the Hall coefficients of the components. Certain terms in formula (A18) correspond to the rotating currents (see Application).

Figure 10 shows results of calculation for the effective relative Hall coefficient (Fig. 10) at the same values of parameters as Eq. (9), however with another value for the parameter $y=0.1$. Hence the Hall coefficient varies smoothly with concentration when $H \simeq 0$, moreover, a jump exists near the percolation threshold when $H \to \infty$ (Fig. 10). The dependence of effective conductivity is roughly the same as Fig. 9. Here we took such values of the Hall properties in order to focus both on effects caused by the fluctuation of density of carriers n and on effects caused by the fluctuation of mobility of carriers μ [Eqs. (8)–(11)].

Fluctuations in the dependence of the effective Hall coefficient exist when the value of the Hall coefficient in the second component is about $R_2 \simeq 10^5 R_1$ if $H \simeq 0$ at $p < p_c$. In the range $p > p_c$ the effective Hall coefficient decreases steadily to the value R_1.

For $H=10^4$ the effective Hall coefficient decreases steadily from R_2 to R_1 in the range $0 < p < p_c$. For $p > p_c$ the effective Hall coefficient is equal to R_1 and does not depend on the concentration. For the given parameters the effective conductivity practically does not depend on the magnetic

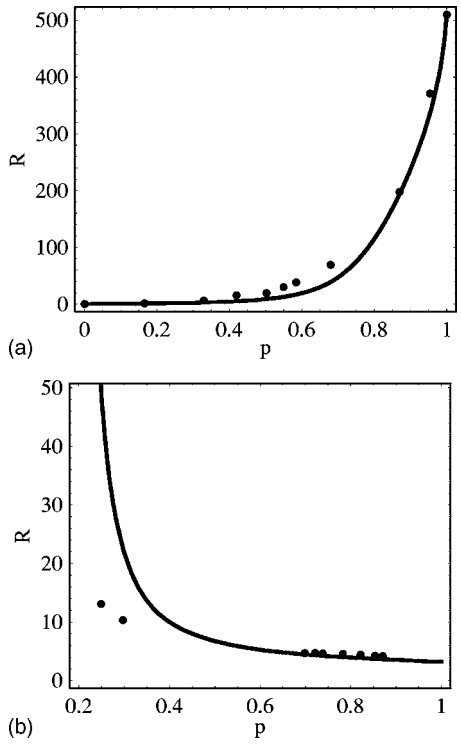

FIG. 11. The comparison between the calculations and the experiments for the dependencies of effective Hall coefficient of composites Bi-Cd (a) and for Na_xWO_3 (b) on the concentration of a phase of one of the components.

field H. Discrepancies in the range $p > p_c$ are unimportant. Figure 11 shows the comparison between the calculation of the effective Hall coefficient and results of two experiments.[26,2]

Fractal properties

Figure 12 shows the dependence of the effective Hall properties of a composite on the scale (the number of iterations which according to Eq. (22) is equal to $n = \ln L_n / \ln l - 1$) near the percolation threshold p_c. According to calculations (Fig. 12), the dependence of the effective Hall properties of a composite on the scale can be divided into two ranges.

For $n < 5$ (Fig. 12), the composite exhibits properties of a fractal object with the characteristic power law dependence of such properties (conductivity σ and Hall coefficient R) on the scale

$$R \sim (L_n)^{\alpha_2}, \quad \alpha_2 \simeq 1.92, \quad n < 5, \quad H \to 0,$$

$$\sigma \sim (L_n)^{\alpha_1}, \quad \alpha_1 \simeq 3.0, \quad n < 5, \quad H \to 0. \qquad (32)$$

For $n > 5$ (Fig. 12) the Hall properties do not depend on the scale, i.e., Euclidean geometry prevails. Here the composite can be described as a quasihomogeneous ("gray") medium, whose properties correspond to the effective values of properties. When $n \simeq 5$, the transformation between a fractal and a quasihomogeneous mode of behavior of Hall properties exists. In other words, the scale $n_\xi = 5$ determines the correlation length ξ.

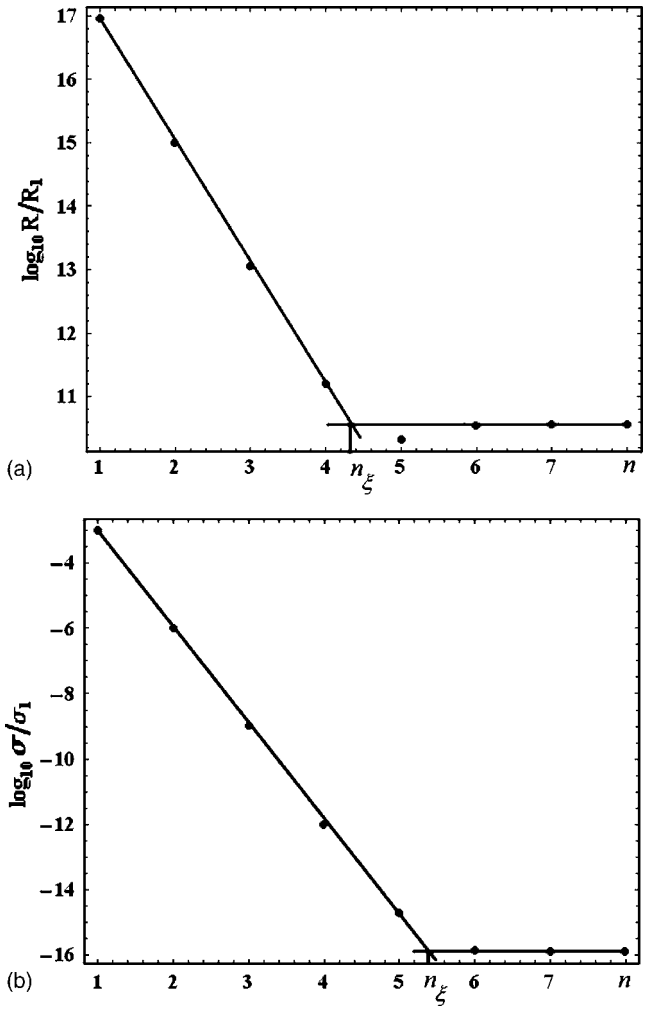

FIG. 12. The dependence of the relative effective Hall coefficient (a) and the relative effective conductivity (b) on a scale.

Note again that the accuracy of calculation by the iterative method for the Hall properties of a 3D composite with chaotic structure depends on the calculation accuracy of probability function $Y(p)$ (probability that the point belongs to the connecting set). The probability function $Y(p)$ describes the random structure of a composite completely in the percolation threshold: it defines the value of the percolation threshold p_c and the correlation length critical exponent ν [Eq. (24)]. The correlation length is a very important characteristic of the composite: it defines the region where the composite exhibits properties of a fractal object: $L_0 < L_n < \xi$. Moreover, the different unit cells possess the different probability functions $Y(p)$. The different values of the critical exponent ν exerts certain influence (essentially near the percolation threshold) on the critical behavior of the Hall parameters. We plan to consider this problem in our future publication.

A rough approximation is the computation of the Hall properties of a connecting set and nonconnecting set based on cube inside cube cell by formulas from the Appendix. Hence our results can be considered as the analysis of qualitative dependencies of the effective Hall properties (Figs. 5–12). In the future we shall calculate the probability

function $Y(p)$ and the Hall properties of the connecting set and nonconnecting set more accurately.

IV. CONCLUSION

The iterative averaging method allows us to study the Hall properties of the composite over a large range of different parameters: concentrations, conductivities, Hall coefficients of components, and a magnetic field.

A number of interesting results have been obtained (due to our fractal model of structure and the iterative averaging method) for the Hall properties of the composite, e.g., the considered logarithmic derivative allows one to obtain the critical exponents for the Hall coefficient (Fig. 8) and conductivity (Fig. 7) for various values of the magnetic field H. When $\sigma_1=\sigma_2$ (Fig. 9) effective conductivity is a constant if $H=0$ and tends to zero if $H\to\infty$ near the percolation threshold. On the left from the percolation threshold ($p<p_c$) the rise of the Hall coefficient is more rapid as the magnetic field increases (Fig. 9). On the right from the percolation threshold ($p>p_c$) the Hall coefficient practically does not depend on the concentration p.

The iterative averaging method allows us to obtain the specific dependencies of the effective Hall properties on a scale (number of iteration steps). This dependence yields information about geometry prevailing at a given scale. The transformation to the regime of Euclidean geometry (quasihomogeneous medium) occurs on a characteristic scale ξ where the logarithm of a property ceases to depend on a scale. Note that the scale ξ, as well as dependencies of the effective Hall properties, is multiparametric dependency.

Our results are more general than the results of the effective medium theory, percolation theory, and perturbation theory, since in our model there are not any small parameters whereas our renormalization function (23) is exact at any value of p.

Our model describes the effective Hall properties of a 3D disordered composite with the same degree of accuracy as the following conditions are applicable to a composite:

(1) conductivity tensor in both components of the composite can be written as Eq. (12);

(2) cube inside a cube cell is suitable for the description of actual composite structure; and

(3) renormalization probability function $Y(p)$ [Eq. (23)] with the percolation threshold p_c is applicable for actual elementary cell.

Our general aims in future publications are the more accurate calculation of the probability function $Y(p)$, a less crude approximation for the model of the elementary cell, and use of different probability functions $Y(p)$ in our calculations in order to illustrate their influence on the critical behavior of the Hall properties of a three-dimensional composite.

APPENDIX

1. Galvanomagnetic properties of cube inside a cube elementary cell

Suppose that the magnetic field $\mathbf{H}$ is directed vertically (along the axis Ox_3) and the current $\langle\mathbf{j}_1\rangle$ is directed horizontally along Ox_1, as shown in Fig. 13. Take the size of the outer cube as 1 and the size of the inner cube as d. The volume concentration and the size of the inner cube are now related by the formula $d=\sqrt[3]{p}$.

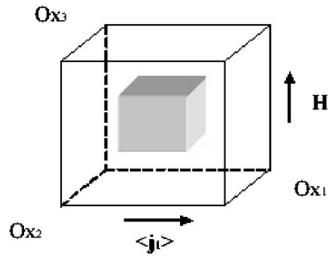

FIG. 13. The "cube inside cube" model.

Ohm's law is then

$$\mathbf{j}=\hat{\sigma}\mathbf{E}, \tag{A1}$$

where

$$\sigma=\begin{pmatrix}\sigma_{11} & \sigma_{12} & 0\\ -\sigma_{12} & \sigma_{22} & 0\\ 0 & 0 & \sigma_{33}\end{pmatrix},\quad \mathbf{E}=\begin{pmatrix}\mathbf{E}_1\\ \mathbf{E}_2\\ \mathbf{E}_3\end{pmatrix},\quad \mathbf{j}=\begin{pmatrix}\mathbf{j}_1\\ \mathbf{j}_2\\ \mathbf{j}_3\end{pmatrix}.$$

We can express this equation as

$$\mathbf{E}=\hat{\rho}\mathbf{j}, \tag{A2}$$

where

$$\rho=\begin{pmatrix}\rho_{11} & -\rho_{12} & 0\\ \rho_{12} & \rho_{22} & 0\\ 0 & 0 & \rho_{33}\end{pmatrix}.$$

Now we carry out a conventional partition of the cube inside a cube cell into layered structures so that it is possible to compose the cell from them. Next we calculate the Hall properties of the cube inside a cube cell approximately by means of step-by-step averaging of Hall properties of layered structures. Hence the approximate evaluation of the Hall properties of the cube inside a cube cell is reduced to the evaluation of the properties of a layered medium (see Fig. 13).

2. Galvanomagnetic properties of layered structures

We shall consider three different cases of orientation for the magnetic field $\mathbf{H}$, current $\langle\mathbf{j}_1\rangle$, and direction of layers (Fig. 14).

a. Orientation a

In this case the layers are parallel to the current $\langle\mathbf{j}_1\rangle$ and perpendicular to the field $\mathbf{H}$. According to Fig. 14(a) the currents and the fields obey the following conditions:

$$\langle\mathbf{j}_1\rangle=p\langle\mathbf{j}_1^{(1)}\rangle+(1-p)\langle\mathbf{j}_1^{(2)}\rangle,$$

$$\langle\mathbf{E}_1\rangle=\langle\mathbf{E}_1^{(1)}\rangle=\langle\mathbf{E}_1^{(2)}\rangle,$$

$$\langle\mathbf{j}_2\rangle=p\langle\mathbf{j}_2^{(1)}\rangle+(1-p)\langle\mathbf{j}_2^{(2)}\rangle,$$

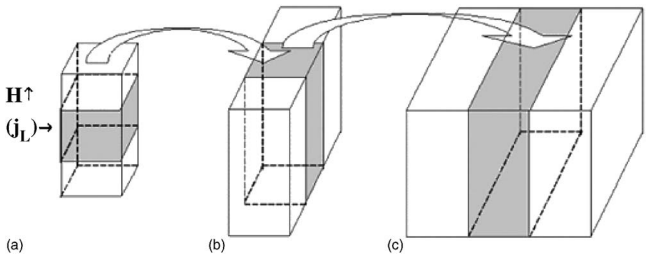

FIG. 14. The layered structure of cube inside a cube cell.

$$\langle \mathbf{E}_2 \rangle = \langle \mathbf{E}_2^{(1)} \rangle = \langle \mathbf{E}_2^{(2)} \rangle, \tag{A3}$$

where angular brackets $\langle\ \rangle$ mean space average [Eq. (5)] and upper index means the content of the layer (first or second component):

$$\langle f \rangle = \frac{1}{V}\int_V f(\mathbf{r})d^3r, \quad \langle f^{(i)} \rangle = \frac{1}{V_i}\int_{V_i} f(\mathbf{r})d^3r. \tag{A4}$$

According to conditions (A3) we will express longitudinal current $\langle \mathbf{j}_1 \rangle$ and Hall current $\langle \mathbf{j}_2 \rangle$ in the first component as follows:

$$\langle \mathbf{j}_1^{(1)} \rangle = \chi_1 \langle \mathbf{j}_1 \rangle,$$

$$\langle \mathbf{j}_2^{(1)} \rangle = \chi_2 \langle \mathbf{j}_1 \rangle, \tag{A5}$$

where

$$\chi_2 = \frac{(p\rho_{11}^{(2)} + (1-p)\rho_{11}^{(1)})\rho_{11}^{(2)} + (p\rho_{12}^{(2)} + (1-p)\rho_{12}^{(1)})\rho_{12}^{(2)}}{(p\rho_{11}^{(2)} + (1-p)\rho_{11}^{(1)})^2 + (p\rho_{12}^{(2)} + (1-p)\rho_{12}^{(1)})^2},$$

$$\chi_1 = \frac{(p\rho_{11}^{(2)} + (1-p)\rho_{11}^{(1)})\rho_{12}^{(2)} + (p\rho_{12}^{(2)} + (1-p)\rho_{12}^{(1)})\rho_{11}^{(2)}}{(p\rho_{11}^{(2)} + (1-p)\rho_{11}^{(1)})^2 + (p\rho_{12}^{(2)} + (1-p)\rho_{12}^{(1)})^2}. \tag{A6}$$

From conditions (A3) it follows that the expression for Hall field $\langle \mathbf{E}_2 \rangle$ in case (a) looks like

$$\langle \mathbf{E}_2 \rangle = \rho_{12}^{(1)} \langle \mathbf{j}_1^{(1)} \rangle + \rho_{11}^{(1)} \langle \mathbf{j}_2^{(1)} \rangle = (\rho_{12}^{(1)}\chi_1 + \rho_{11}^{(1)}\chi_2)\langle \mathbf{j}_1 \rangle. \tag{A7}$$

The expression in parentheses is nondiagonal element $\rho_{12}^{(a)}$ of tensor $\hat{\rho}$. For case (a) it looks like

$$\rho_{12}^{(a)} = \rho_{12}^{(1)}\chi_1 + \rho_{11}^{(1)}\chi_2. \tag{A8}$$

From conditions (A3) and from law (A2) it follows that the longitudinal field $\langle \mathbf{E}_1 \rangle$ in case (a) is equal to

$$\langle \mathbf{E}_1 \rangle = \rho_{11}^{(1)} \langle \mathbf{j}_1^{(1)} \rangle - \rho_{12}^{(1)} \langle \mathbf{j}_2^{(1)} \rangle = (\rho_{11}^{(1)}\chi_1 - \rho_{12}^{(1)}\chi_2)\langle \mathbf{j}_1 \rangle. \tag{A9}$$

The expression in parentheses is diagonal element $\rho_{11}^{(a)}$ of tensor $\hat{\rho}$. For case (a) it looks like

$$\rho_{11}^{(a)} = \rho_{11}^{(1)}\chi_1 - \rho_{12}^{(1)}\chi_2. \tag{A10}$$

b. Orientation b

In this case the layers are parallel to the current $\langle \mathbf{j}_1 \rangle$ and parallel to the field $\mathbf{H}$. According to Fig. 14(b) currents and fields obey the following conditions:

$$\langle \mathbf{j}_1 \rangle = \langle \mathbf{j}_1^{(a)} \rangle = \langle \mathbf{j}_1^{(2)} \rangle,$$

$$\langle \mathbf{E}_1 \rangle = p\langle \mathbf{E}_1^{(a)} \rangle + (1-p)\langle \mathbf{E}_1^{(2)} \rangle,$$

$$\langle \mathbf{j}_2 \rangle = p\langle \mathbf{j}_2^{(a)} \rangle + (1-p)\langle \mathbf{j}_2^{(2)} \rangle,$$

$$\langle \mathbf{E}_2 \rangle = \langle \mathbf{E}_2^{(a)} \rangle = \langle \mathbf{E}_2^{(2)} \rangle. \tag{A11}$$

From now on the alphabetic upper indexes specify that the fields and currents belong to the corresponding region. As we can see in Fig. 14, the area (a) in case (b) is just a layer with averaged properties (A8) and (A10).

According to conditions (A11) we will express the Hall current $\langle \mathbf{j}_2 \rangle$ in the layer (a) as follows:

$$\langle \mathbf{j}_2^{(a)} \rangle = \chi_3 \langle \mathbf{j}_1 \rangle, \tag{A12}$$

where

$$\chi_3 = \frac{(1-p)(\rho_{12}^{(2)} - \rho_{12}^{(a)})}{p(\rho_{11}^{(a)} + \rho_{11}^{(2)})}. \tag{A13}$$

From conditions (A11) and from law (A2), it follows that Hall field $\langle \mathbf{E}_2 \rangle$ in case (b) is equal to

$$\langle \mathbf{E}_2 \rangle = \rho_{12}^{(a)} \langle \mathbf{j}_1^{(a)} \rangle + \rho_{11}^{(a)} \langle \mathbf{j}_2^{(a)} \rangle = (\rho_{12}^{(a)} + \rho_{11}^{(a)}\chi_3)\langle \mathbf{j}_1 \rangle. \tag{A14}$$

The expression in parentheses in Eq. (A14) is nondiagonal element $\rho_{12}^{(a)}$ of tensor $\hat{\rho}$ for case (b):

$$\rho_{12}^{(b)} = \rho_{12}^{(a)} + \rho_{11}^{(a)}\chi_3. \tag{A15}$$

From conditions (A11), it follows that the expression for longitudinal field $\langle \mathbf{E}_1 \rangle$ in case (b) looks as follows:

$$\langle \mathbf{E}_1 \rangle = p\langle \mathbf{E}_1^{(a)} \rangle + (1-p)\langle \mathbf{E}_1^{(2)} \rangle = p(\rho_{11}^{(a)}\langle \mathbf{j}_1 \rangle - \rho_{12}^{(a)}\langle \mathbf{j}_2^{(a)} \rangle) + (1-p)(\rho_{11}^{(2)}\langle \mathbf{j}_1 \rangle - \rho_{12}^{(2)}\langle \mathbf{j}_2^{(2)} \rangle). \tag{A16}$$

According to conditions (A11), we will express the Hall currents as follows:

$$\langle \mathbf{j}_2^{(a)} \rangle = \frac{\rho_{12}^{(b)} - \rho_{12}^{(a)}}{\rho_{11}^{(a)}}\langle \mathbf{j}_1 \rangle,$$

$$\langle \mathbf{j}_2^{(2)} \rangle = \frac{\rho_{12}^{(b)} - \rho_{12}^{(2)}}{\rho_{11}^{(2)}}\langle \mathbf{j}_1 \rangle. \tag{A17}$$

From Eqs. (A16) and (A17), it follows that $\langle \mathbf{E}_1 \rangle = (\cdots) \times \langle \mathbf{j}_1 \rangle$ and diagonal element $\rho_{11}^{(b)}$ of tensor $\hat{\rho}$ for case (b) is equal to

$$\rho_{11}^{(b)} = p\left[\rho_{11}^{(a)} - \rho_{12}^{(a)}\frac{\rho_{12}^{(b)} - \rho_{12}^{(a)}}{\rho_{11}^{(a)}}\right] + (1-p)\left[\rho_{11}^{(2)} - \rho_{12}^{(2)}\frac{\rho_{12}^{(b)} - \rho_{12}^{(2)}}{\rho_{11}^{(2)}}\right]. \tag{A18}$$

As $\rho_{12} = RH$, from Eq. (A18) it follows that the ohmic resistivity $\rho_{11}^{(b)} \sim H^2$. Hence the existence of dependence on a field is defined by a difference between Hall coefficients $(R_1 - R_2)$ of components. If this difference is not equal to

zero ($R_1 \neq R_2$), at a composite there are rotational Hall currents. These currents give the contribution to the ohmic resistivity (and to the ohmic conductivity, respectively) which depends on a magnetic field H. Hence if there are even small inhomogeneities in the substance, then the "saturation" ($\rho_{11} \rightarrow \rho_\infty$, $H \rightarrow \infty$) does not appear for the ohmic resistance with the increase of a magnetic field.

c. Orientation c

In this case the layers are parallel to the current $\langle \mathbf{j}_1 \rangle$ and perpendicular to the field $\mathbf{H}$. According to Fig. 14(c) the currents and the fields obey the following conditions:

$$\langle \mathbf{j}_1 \rangle = p\langle \mathbf{j}_1^{(b)} \rangle + (1-p)\langle \mathbf{j}_1^{(2)} \rangle,$$

$$\langle \mathbf{E}_1 \rangle = \langle \mathbf{E}_1^{(b)} \rangle = \langle \mathbf{E}_1^{(2)} \rangle,$$

$$\langle \mathbf{j}_2 \rangle = \langle \mathbf{j}_2^{(b)} \rangle = \langle \mathbf{j}_2^{(2)} \rangle,$$

$$\langle \mathbf{E}_2 \rangle = p\langle \mathbf{E}_2^{(b)} \rangle + (1-p)\langle \mathbf{E}_2^{(2)} \rangle. \tag{A19}$$

According to conditions (A19) we shall express the longitudinal current $\langle \mathbf{j}_1 \rangle$ in the layer "b" as follows:

$$\langle \mathbf{j}_1^{(b)} \rangle = \chi_4 \langle \mathbf{j}_1 \rangle, \tag{A20}$$

where

$$\chi_4 = \frac{\rho_{11}^{(2)}}{(1-p)\rho_{11}^{(b)} + p\rho_{11}^{(2)}}. \tag{A21}$$

From conditions (A19) and from expression (A20), it follows that expression for the Hall field $\langle \mathbf{E}_2 \rangle$ in case (c) looks like

$$\langle \mathbf{E}_2 \rangle = p\rho_{12}^{(b)}\langle \mathbf{j}_1^{(b)} \rangle + (1-p)\rho_{12}^{(2)}\langle \mathbf{j}_1^{(2)} \rangle$$
$$= (\chi_4 p\rho_{12}^{(b)} + \chi_4(1-p)\rho_{12}^{(2)})\langle \mathbf{j}_1 \rangle. \tag{A22}$$

The expression in parentheses in Eq. (A19) is the nondiagonal element $\rho_{12}^{(a)}$ of tensor $\hat{\rho}$ for case (c), i.e., for the whole "cube inside cube" cell:

$$\rho_{12}^{(c)} = \chi_4[p\rho_{12}^{(b)} + (1-p)\rho_{12}^{(2)}]. \tag{A23}$$

From conditions (A19) it follows that the expression for longitudinal field $\langle \mathbf{E}_1 \rangle$ in case (c) looks like

$$\langle \mathbf{E}_1 \rangle = \rho_{11}^{(b)}\langle \mathbf{j}_1 \rangle - \rho_{12}^{(b)}\langle \mathbf{j}_2^{(b)} \rangle = \rho_{11}^{(b)}\chi_4\langle \mathbf{j}_1 \rangle, \tag{A24}$$

i.e.,

$$\rho_{11}^{(c)} = \rho_{11}^{(b)}\chi_4 = \rho_{11}^{(b)}\frac{\rho_{11}^{(2)}}{(1-p)\rho_{11}^{(b)} + p\rho_{11}^{(2)}}. \tag{A25}$$

Note that the case shown in Fig. 13 corresponds to nonconnecting set structure and expressions (A23) and (A25) describe the average properties of a nonconnecting set. To obtain similar expressions for connecting set structure, it is necessary in all the calculations of the Appendix to make consistent the change of variables:

$$\rho_{11}^{(i)} \rightarrow \rho_{11}^{(j)}, \quad \rho_{12}^{(i)} \rightarrow \rho_{12}^{(j)},$$

$$p \rightarrow (1-p), \quad i,j = 1,2. \tag{A26}$$

As a result we shall obtain the expressions similar to Eqs. (A23) and (A25), but for a connecting set structure. These expressions are also used for calculation of the effective Hall properties of 3D composite.

[1] B. I. Shklovskii, Zh. Eksp. Teor. Fiz. **72**, 288 (1977) [Sov. Phys. JETP **45**, 152 (1977)].
[2] I. Webman, J. Jortner, and M. H. Cohen, Phys. Rev. B **13**, 713 (1976).
[3] C. Herring, J. Appl. Phys. **31**, 1939 (1960).
[4] Y. A. Dreizin and A. M. Dykhne, Zh. Eksp. Teor. Fiz. **63**, 242 (1972) [Sov. Phys. JETP **36**, 127 (1973)].
[5] J. B. Keller, J. Math. Phys. **5**, 548 (1964).
[6] A. M. Dykhne, Zh. Eksp. Teor. Fiz. **59**, 641 (1970) [Sov. Phys. JETP **32**, 348 (1971)].
[7] Y. M. Strelniker and D. J. Bergman, Phys. Rev. B **61**, 6288 (2000).
[8] B. Y. Balagurov, Fiz. Tverd. Tela (Leningrad) **20**, 3332 (1978) [Sov. Phys. Solid State **20**, 1922 (1978)].
[9] H. Christiansson, Phys. Rev. B **56**, 572 (1997).
[10] S. A. Bulgadaev, Pis'ma Zh. Eksp. Teor. Fiz. **77**, 615 (2003).
[11] I. Ruzin and S. Feng, Phys. Rev. Lett. **74**, 154 (1995).
[12] S. Kirkpatrick, Rev. Mod. Phys. **45**, 574 (1973).
[13] D. J. Bergman, Y. Kantor, D. Stroud, and I. Webman, Phys. Rev. Lett. **50**, 1512 (1983).
[14] D. Adler, L. P. Flora, and S. D. Senturia, Solid State Commun. **12**, 9 (1973).
[15] D. J. Bergman and D. Stroud, Phys. Rev. B **32**, 6097 (1985).
[16] D. J. Bergman and D. G. Stroud, Phys. Rev. B **62**, 6603 (2000).
[17] G. G. Batrouni, A. Hansen, and B. Larson, Phys. Rev. E **53**, 2292 (1996).
[18] J. Bernasconi, Phys. Rev. B **18**, 2185 (1978).
[19] M. B. Heaney, Phys. Rev. B **52**, 12477 (1995).
[20] Y. P. Pellegrini and M. Barthelemy, Phys. Rev. E **61**, 3547 (2000).
[21] S. A. Korzh, Zh. Eksp. Teor. Fiz. **59**, 510 (1970).
[22] I. M. Kaganova, Phys. Lett. A **312**, 108 (2003).
[23] D. Staufer and A. Aharony, *Introduction to Percolation Theory*, 2nd ed. (Taylor and Francis, London, 1994).
[24] M. Sahimi, *Heterogeneous Materials (Volume I, Linear Transport and Optical Properties; Volume II, Nonlinear and Breakdown Properties and Atomistic Modeling*) (Springer, New York, 2003).
[25] E. Feder, *Fractals* (translated into Russian) (Nauka, Moscow, 1999), p. 260.
[26] W. R. Thomas and E. Evans, Philos. Mag. **16**, 329 (1933).